International Journal of Scientific Engineering and Technology (ISSN : 2277-1581)
www.ijset.com, Volume No.1, Issue No.4, pg : 76-88 01 Oct. 2012

Air Curtain Design Optimization of Refrigerated Vertical Display Cabinet using CFD

Abas F Hadawey[1*], Tawfiq J. Jaber[2], Waleed Abdul Ghaffar[3], A.H.A.M. Hasan[4]
[1, 3, 4] Mechanical and Industrial Engineering, Caledonian College of Engineering in Oman, Affiliated to Glasgow Caledonian University in Scotland UK
[2] Mechanical and industrial Engineering Dept., Faculty of Engineering and Applied Sciences, Alhosn University, Abu Dhabi, UAE
Email: abas@caledonian.edu.om

Abstract

This paper presents computational investigations to address some of the design parameters that have significant effects on the performance of the refrigerated display cabinets. These parameters include air curtain velocity, width, discharge angle and positioning of the air curtain outlet from the front edge of the top shelf, also the effect of using a honeycomb on the flow path at the air curtain outlet.

A 3D CFD model was constructed to assess the effect of the side flow on the performance of the vertical display cabinet. The suitability of using 2D CFD to carry out the display cabinet design optimisation was also considered.

Experimental work was then carried out to validate the numerical work: there was good agreement between the data generated from the numerical work with the experimental results.It was determined that for the length of the cabinet considered in this investigation, the flow can be assumed to be two-dimensional, for most of the cabinet length.

The results also indicate that optimum air curtain mass flow rate should account for nearly a third of the total air mass flow rate inside the display cabinet.

Key words

Air curtain, refrigerated multi-deck display cabinet, computational fluid dynamics CFD

1. Introduction

Vertical multi-deck display cabinets (found commonly in supermarkets), are large consumers of electrical energy because of their negative interaction with the ambient environment. Air curtains are widely used in refrigerated display cabinets to reduce the air, thermal and moisture transfer between the conditioned environment (inside the cabinet) and the surrounding ambient. Hence, the design of an energy efficient display cabinet is a much desired research topic. If display cabinets can be designed to maintain specific boundary conditions under different operating conditions then the displayed food will have longer shelf life, be maintained at a higher quality, and refrigeration operating costs can be substantially reduced by retailers, and product wastage reduced. Open refrigerated display cabinets are designed to allow the customer unrestricted access to the displayed product. Products are cooled by air circulating through an evaporator, which is cooled, and passed vertically upwards through a perforated back-panel. The air curtain in the display cabinet is designed to provide a barrier between the environment inside the cabinet and the surrounding air outside [1]. Perforated back-panel directs the cooled air to the shelves and across the products maintaining the desired temperature. Interaction through the air curtain flow between the warm air coming from outside the cabinet and cold air coming from the shelves cannot be avoided. Part of this combination flow is drawn into the evaporator to cycle around again and the other part spills over the display cabinet. The amount of warm air that moves into the display cabinet through the air curtain and to the return air grill is called the infiltration load. The infiltration load has two components; sensible and latent.

The sensible portion refers to the direct temperature-driven heat added to the display case. The latent portion refers to the heat content of the moisture added to the cabinet by the surrounding air drawn into the cabinet through the air curtain. Open display cabinets are commonly used for chilled food, and vertical display cabinets are the preferred type. The open design and a wide display area make the control of energy consumption and control of the correct food storage temperature particularly critical. In fact, it has been demonstrated that air infiltration through the front opening of the cabinet can be up to 60-70 % of the total load on the heat exchanger (and the cost of refrigeration) from the ambient in vertical display cabinets [2].It was reported in the UK that sales of chilled food in retail outlets in 2003, amounted to about £7.68 billion [3] (and is growing at about 3.5% pa). Being able to retain the temperature of this food is of great important to retailers to ensure optimal food quality, safety and shelf life. Hadawey [4] reported that by reducing the display temperature by 1K, in the range of 277 to 280K , the storage life of some types of meat (unwrapped) can be extended by around 10 hours. As a result of the interaction of the air curtain flow with ambient air, a more or less significant amount of ambient air is always entrained, reducing the temperature control ability and affecting the performance of the display cabinet. Therefore, despite the improvements made in the last two and half decades, a better design of retail cabinets is still an essential target for the refrigeration industry. Consequently, numerical methods for predicting the cabinet performance are of a great interest, since the numerical procedure is time effective.

Considering every single part of the display cabinet in the model will provide more accurate results i.e. the perforated back-panel, top ceiling gap and the configuration of the air curtain, where it has been reported that the velocity distribution at the air curtain outlet has considerable effect on the cooling load of the display cabinet. Hadawey [4] found that using a modified shape honeycomb at the air curtain outlet will provide uniform velocity at this point and can achieve a 4.7% saving in the cooling load of the display cabinet. Moreover, the air distribution in the display cabinet playing important role of controlling the performance of the display cabinet. [21] reported that 70-30 distribution of flow between the air curtain and the rear duct perforation yields a performance that satisfies the standards of the operation of the display cabinet.

Parts such as the evaporator of the display cabinet are a complex task to model, involving the air velocity, load temperature distribution, frost formation and the characteristics of the flow through the evaporator section, which requires a dynamic CFD model [5].

Furthermore the influences of the external conditions are important. In order to investigate the performance of the display cabinet, the test should meet the terms of the standard test conditions, which state that airflow with a velocity of 0.18-0.2 m/s should be present parallel to the longitudinal axis of the cabinet [6]. For this reason, simplified models are usually employed for the investigation of display cabinet design optimisation.

In spite of it being recognized that 3D CFD modelling effects can affect the cabinet performance, almost all of the CFD simulations available in the literature are performed in 2D, implemented on the median section of the cabinet such as [2-7-10] and they showed the CFD modelling to be a valuable tool in rapidly providing design options to improve the air flow within the display cabinet. Very little information is available in the literature with regard to the analysis of the impact of a 3D flow on the cabinet performance. [2] found that 3D simulations of the vertical display cabinet to be a reliable tool for the prediction of the air curtain flow pattern and thus generate more reliable results.

This paper describes investigations carried out for the design optimization of vertical display cabinets, i.e. the combination of air curtain configuration, velocity and temperature that leads to better display cabinet performance.

Assessment of the suitability of using a 2D CFD model to carry out the display cabinet design optimization is also considered in this investigation.

2. Experimental work and standard test

The main aims of the experimental investigation was to identify the temperature distribution of the product inside the display cabinet, air temperature, air velocity and relative humidity of the air entering (air-on) and leaving (air-off) the evaporator within the display cabinet. The experimental results delivered data that used as input to the CFD model and later be compared with the results of the simulation to asses the accuracy and validity of the established CFD model.

A Carter multi-deck display cabinet was used in this investigation. The cabinet Figure 1 is 2.45m long with a single air curtain. The cabinet was designed to meet the requirements of class M0 (Product temperature range –1 °C to 4°C). The display unit consists of a shelving system with an evaporator mounted in its base.

The air curtain is situated at the top of the display and the flow passes through to the base through a return grill located in the top of the front stand. The air curtain width and discharge angle are 110 mm and 12° respectively, the back-panel width and top ceiling gap are 40mm and 65mm respectively Figure 2. Three evaporator fans were installed to provide the required air to the cabinet, the air mass flow rate was around 0.28 (kg/s).

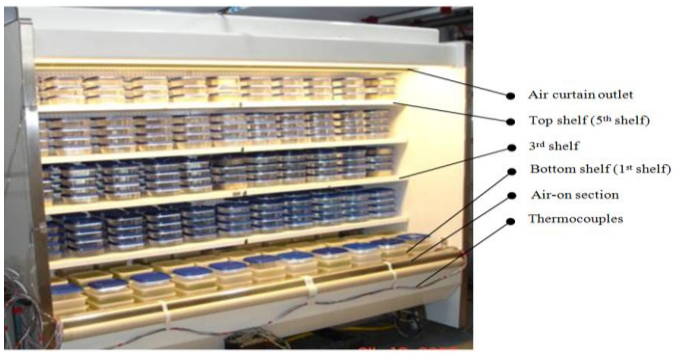

Figure 1: A vertical open display cabinet

A typical back-panel continues further upwards and across the ceiling to allow a proportion of air to exit finally through the air curtain outlet. This generates a protective air curtain down the front of the shelves.

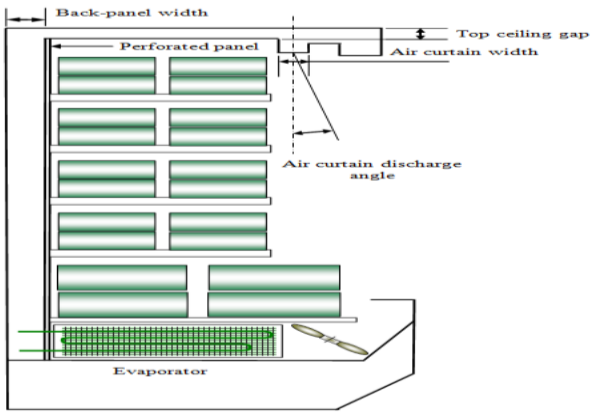

Figure 2: Cross section of the vertical display cabinet (side view)

The refrigeration to the display cabinet was driven by an absorption chillier with propylene Glycol/water mixture (33% by volume) as a heat transfer fluid. The chiller mass flow rate was 0.8 (m^3/h). The supply glycol temperature was around -5°C. The tests were carried out in a test room conforming to EN441 standard and controlled to climate class III (temperature of 25°C and relative humidity of 60%), [11].

The cabinet was loaded according to EN441 specifications [11]. M-packs (composed of 30% cellulose, 70% water and salt), which had a calibrated T-type thermocouple inserted into the geometric centre of the pack, were used at the positions where product temperature needed to be measured. The rest of the cabinet was loaded with water containers to provide thermal capacity.

Product temperatures were collected from the bottom (shelf 1), third (shelf 3) and top (shelf 5) shelves at three different sections (left, right and central) in the front and rear of each shelf Figure 3. The left and right sections were 200 mm away from both side panels of the display cabinet. Air measurements were also collected in the evaporator coil air-off & on sections.

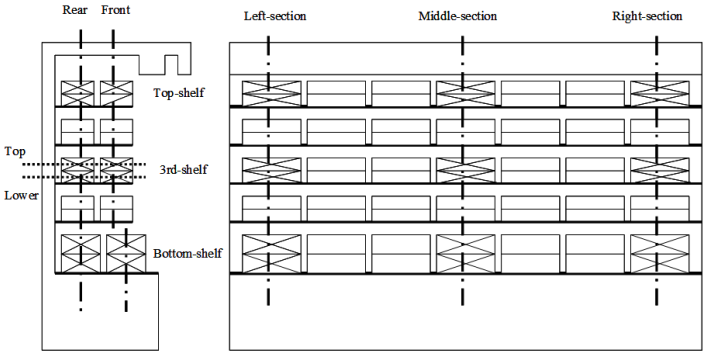

Figure 3: The cabinet loading pattern

A computer-based data logging system was used to record the data (Data-scan Analog Measurement Processors 7320- limits of error 0.3°C). The data acquisition hardware is located externally and linked to the computer for communication purposes. Labtech Control is a window-based icon driven data acquisition software that records the data into files are compatible with the data acquisition hardware.

3. Modelling the vertical display cabinet

The airflow patterns and temperature distributions within the refrigerated display cabinet were modelled using FLUENT computer simulation software. A 3-D and 2-D CFD models were created using Fluent to model the display cabinet, this software is designed to analyse the flow and thermal distribution in enclosed spaces.

Computational Fluid Dynamics CFD is the analytical methodology upon which the FLUENT simulation package is based. Fluent utilises the Navier-Stokes equations to describe fluid flow and energy equation to describe temperature distribution.

For the 3D CFD model, FLUENT solves for the five variables: u, v, w, which are the x, y, and z components of the fluid velocity, respectively, as well as the pressure, p, and temperature, T, of the fluid and/or solid materials. All of these variables are functions of x, y, z and time.

Continuity Equation:

$$\frac{\partial u}{\partial x}+\frac{\partial v}{\partial y}+\frac{\partial w}{\partial z}=0 \tag{1}$$

Momentum Equations (Navier-Stokes):

$$\rho\left(\frac{\partial u}{\partial t}+u\frac{\partial u}{\partial x}+v\frac{\partial u}{\partial y}+w\frac{\partial u}{dz}\right)= -\frac{\partial p}{\partial x}+\mu\left(\frac{\partial^2 u}{\partial x^2}+\frac{\partial^2 u}{\partial y^2}+\frac{\partial^2 u}{\partial z^2}\right)+X \tag{2}$$

$$\rho\left(\frac{\partial v}{\partial t}+u\frac{\partial v}{\partial x}+v\frac{\partial v}{\partial y}+w\frac{\partial v}{dz}\right)= -\frac{\partial p}{\partial y}+\mu\left(\frac{\partial^2 v}{\partial x^2}+\frac{\partial^2 v}{\partial y^2}+\frac{\partial^2 v}{\partial z^2}\right)+Y \tag{2}$$

$$\rho\left(\frac{\partial w}{\partial t}+u\frac{\partial w}{\partial x}+v\frac{\partial w}{\partial y}+w\frac{\partial w}{dz}\right)= -\frac{\partial p}{\partial z}+\mu\left(\frac{\partial^2 w}{\partial x^2}+\frac{\partial^2 w}{\partial y^2}+\frac{\partial^2 w}{\partial z^2}\right)+Z \tag{3}$$

Energy Equation:

$$\rho c_p\left(u\frac{\partial T}{\partial x}+v\frac{\partial T}{\partial y}+w\frac{\partial T}{\partial z}+\frac{\partial T}{\partial t}\right)= -\left(\frac{\partial}{\partial x}(q_x)+\frac{\partial}{\partial y}(q_y)+\frac{\partial}{\partial z}(q_z)\right)+q''' \tag{4}$$

The variations in the z direction in equations (1) to (5) were eliminated when conducting the 2D CFD modelling.

The radiation heat transfer between the display cabinet and the surrounding environment was considered in this study (in a similar manner to [12]) by using the DTRM radiation model.

A turbulence model $(k-\varepsilon)$ was used because it shows a good agreement between the numerical and experimental results. The evaporator section was not considered in the CFD model. The flow at the evaporator outlet (evaporator coil air-off section) was assumed to have uniform distribution.

The 3D model was used to investigate the cross-flow effect. A 2D model was then created to optimize the design of the display cabinet.

4. Grid dependency analysis

Sufficient mesh resolution within critical flow regions has as vast impact in ensuring the stability and convergence of the numerical procedure. It also significantly affects the accuracy of the final computational solution. Therefore, it is desirable that a grid independent study is performed. Since unstructured mesh was used to mesh the 2D & 3D CFD display cabinet models, the grid dependency check was carried out using adaption.

Adapting the grid is a feature available in Fluent, which allows automatic refinement of the grid to better resolve the flow details. The advantage of adaption is that it can be implemented in selected regions of the flow-field. It involves running the CFD model with an initial grid density to convergence. The model then identifies areas of high temperature gradients in the flow field and automatically adapts the grid density in these areas until the solution shows no changes with grid density.

Figure 4 shows the grid density for the 2D CFD model before and after the adapting (the highlighted areas shows where the mesh refinements are implemented).

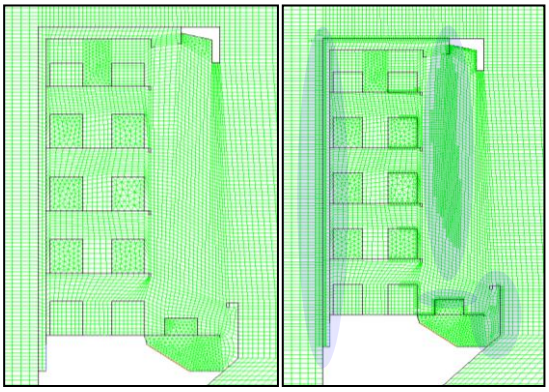

Figure 4: 2D CFD mesh before and after the adaption

The mesh refinement (adaption) was carried out with different temperature gradient and the equivalent cooling load was evaluated.

Figure 5 shows the variation of the cooling load for the 2D & 3D CFD models in the company of the number of cells for refinement. The cooling load of the 2D CFD model was reduced slightly as the number of the cells for refinement increased. After specific number, the cooling load was nearly constant. The first increment in the number of the cells for refinement that provide a constant value of the cooling load was considered as a final mesh for the 2D CFD model. The same procedure was used for the 3D CFD model. Final grid density for the 2D and 3D CFD models were 12192 and 587397 cell respectively.

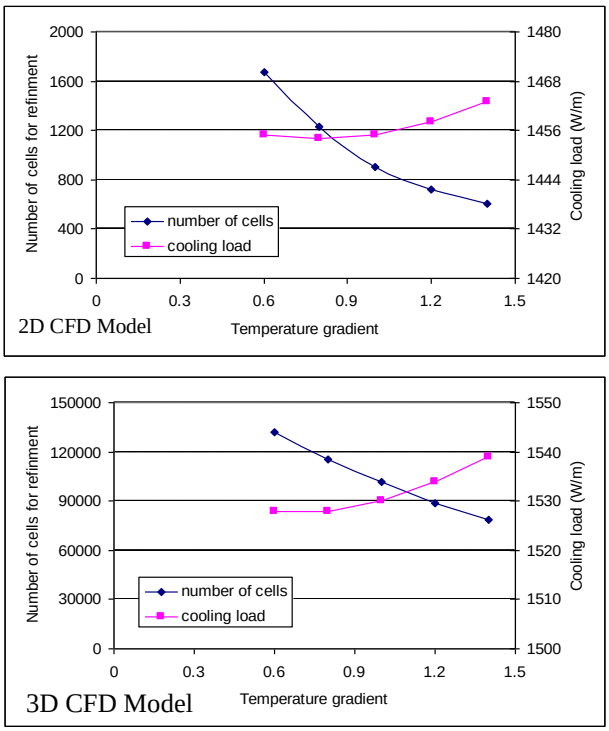

Figure 5: Cooling load variation as a function of the number of cell for refinement for 2D & 3D CFD models

5. Comparisons between CFD prediction and experimental results

The simulated results of the 3D and 2D CFD models of product temperature were compared with the experimental results. Moreover, comparison of the actual cooling load of the display cabinet with the cooling load predicted by the CFD models was also made. The results showed that front product temperature is higher compared to the rear product. Therefore, front product temperature will be only considered in the simulations, Table 1.

Table 1: Comparison of the CFD 3D results with the experimental data

Top Shelf (shelf 5)		Right section	Central section	Left section
		Front	Front	Front
Experimental	top	4.9	5	6.7
	lower	5.4	5.5	6.4
3D CFD	top	4.4	4.1	4.3
	lower	4.1	4.1	4.1
Third Shelf (shelf 3)				
Experimental	top	5.7	5.7	5.5
	lower	5	5	5
3D CFD	top	4.8	5.4	5.5
	lower	4.9	5	5
Bottom Shelf (shelf 1)				
Experimental	top	4.7	6.7	8.5
	lower	4.1	4.7	8.5
3D CFD	top	4.3	6.3	8.1
	lower	4.2	5.8	8.1

It can be seen that the 3D CFD display cabinet model can predict the product temperature well. The maximum difference between the experimental data and the 3D CFD

results was found to be around 2°C on the front left top shelf, and the minimum around 1°C on the lower front bottom shelf. In general the 3D CFD model was able to predict the product temperature with an average error of 7%, see Figure 6.

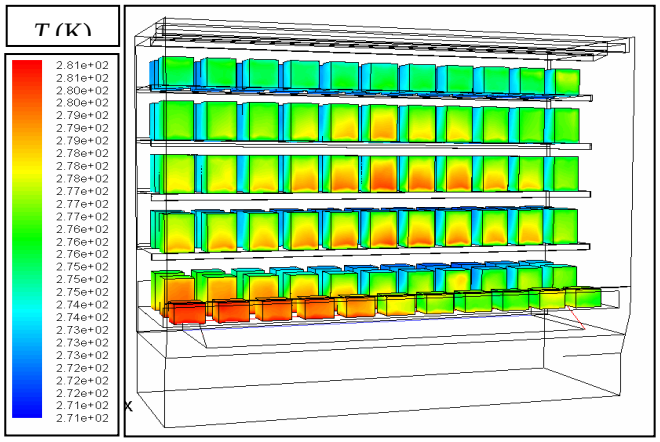

Figure 6: Product temperature distribution as predicted by the 3D- CFD model

The product temperatures collected from the display cabinet showed a variation from the right to the left section and the data collected in the central section closely reflects the average of that variation. Accordingly, the air measurements at the central section of the display cabinet were used as inputs for the 2D CFD model and the collected product temperature data at the central section were used to validate the 2D model.

The average of top and lower product temperature was considered in the simulation of the 2D model. Table 2 shows the comparison between the 2D& 3D CFD results and experimental results.

Table 2: Comparison of the CFD 3D & 2D average product temperature with the experimental data

Parameter	Experimental (W/m)	2D CFD (W/m)	3D CFD (W/m)
Sensible load	930	857	905
Latent load	688	598	623
Total load	1618	1455	1528

It can be seen that the product temperatures predicted by the 2D CFD model are slightly lower than those predicted by the 3D model. This is because of the absence of the cross-flow in the 2D model and the 2D model neglects the heat transfer from the side panels of the display cabinet.

Table 3 shows the cooling load components obtained by the CFD models for the display cabinet. The cooling load components obtained by the 2D model are slightly lower than the cooling load components obtained by the 3D model. The percentage error of the 2D model for predicting the cooling load is 9%.

Table 3: Comparison of the CFD 3D & 2D cooling load with the experimental data

Central section	Shelf 1 Front	Shelf 3 Front	Shelf 5 Front
Experimental	5.7	5.3	5.2
3D CFD	6.1	5.2	4.1
2D CFD	5.8	4.9	4

6. CFD modelling of the honeycomb and the perforated back-panel

Air leaving the display cabinet's evaporator flows through the perforated back-panel to the top ceiling gap and through the air curtain outlet to form an air curtain that provide a barrier to separate the cold environment from the ambient warm air. Some of the air that flows through the back-panel will pass through small holes to the shelves to cool the product. There is little information available in the literature with regard to CFD modelling of the honeycomb and no information is available with regard to the perforated plate of the back-panel of the display cabinet. [13], used a porous media model to model the perforated back-panel and the honeycomb of the air curtain, the same procedures was implemented by [12].

In this investigation the porous media model was used to model the honeycomb and the same model inputs of [13] were used. Since the thickness of the perforated plate of the perforated back-panel for the cabinet considered is 0.9 mm it was difficult to consider the porous media model for modelling the perforated plate. Instead, the porous jump model was implemented because modelling the small scale geometry of the holes on the perforated back-panel section within the overall large scale model of the display cabinet would require an impractically large number of cells. The perforation format of the back-panel can be seen in Figure 7.

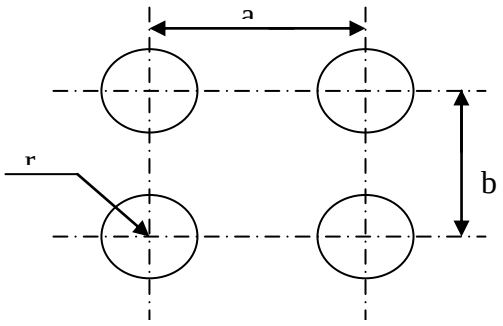

Figure 7: Perforation format of the back-panel

The perforation rate can be calculated as following:

$$perforation \quad rate = \frac{total\ opening\ area\ of\ panel}{total\ area\ of\ panel} = \frac{3.14 \cdot r^2}{a \cdot b} \qquad (5)$$

The experimental procedure for finding the inputs of the porous jump model involved finding the air curtain mass flow rate for different perforation rates at constant total air mass flow rate. Then, from the CFD model, by trial and error, inputs of porous jump model were established equivalent to each perforation rate for 2D and 3D CFD models.

7. Assessing the suitability of using a 2D CFD model for cabinet design optimization

One of the most important points considered in modelling the refrigerated display cabinet is whether the display cabinet should be modelled in 2D or 3D. In supermarkets and shops, display cabinets are subjected to the influence of indoor air motion, and to account for this, test standards require airflow across the face of the display cabinet with a velocity of 0.2 m/s. Previous work carried out by [13-16], on the study of display cabinet performance were based on 2D modelling.

In order to assess the suitability of a 2D model for cabinet design optimization, the cabinet was first modelled in 3D to investigate the effect of the side flow on the cabinet performance along its length. The measured data were used as inputs to the CFD model.

The CFD results showed that path lines of the air curtain flow for a side flow velocity of 0.07 m/s had a uniform distribution for the flow of the air curtain outlet returning to the return air grille. The air curtain was able to cover most of the opening area of the cabinet. Moreover, spillage from the cabinet near the front wall of the cabinet was minimal.

When side flow of 0.2 m/s was applied, the path lines of the air curtain were observed to be affected on the right hand side of the cabinet close to the side panel, where the cross flow was coming from, Figure 8**.**

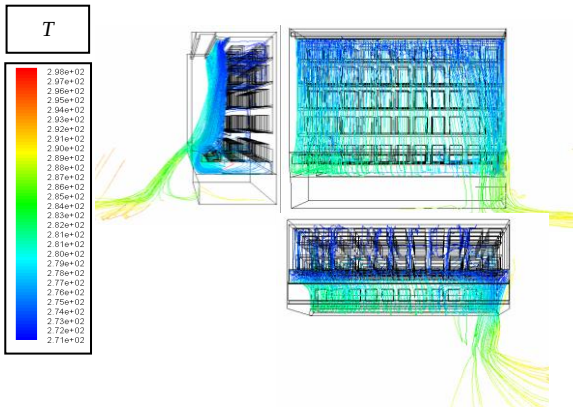

Figure 8: Path lines of air curtain coloured by static temperature with 0.2 m/s cross flow

The CFD results showed that the side flow creates a recirculation area close to the side panel, which in turn creates an area of low pressure close to the air curtain .The low-pressure area "pulls" the air curtain outwards away from the cabinet, and this reduces its effectiveness.

To provide better understanding of the effect of the side flow on the air curtain flow, velocity vectors were plotted at different planes above the floor as shown in Figure 9**.**

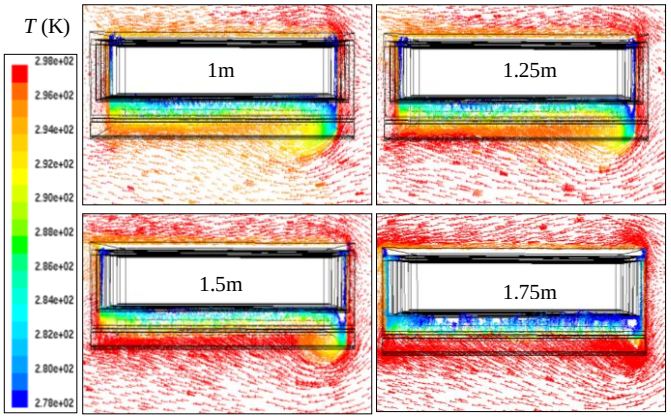

Figure 9: Top-view velocity vectors coloured by static temperature for different planes above the floor

It can be seen that the effect of the cross flow on the display cabinet's air flow pattern remains localised and close to the side panel. It can also be seen that the effect of the side flow is lower at the upper part of the cabinet. This is because the air curtain is stronger in this region and can resist better the influence of the side flow.

It can also be seen from Figure 9 that the side flow only influenced relatively a small section of the display cabinet. This is shown more clearly in Figure 10, which presents temperature contours at different sections along the length of the display cabinet. It can be seen that the effect of the side flow extends up to around 0.4 m of the length of the display cabinet.

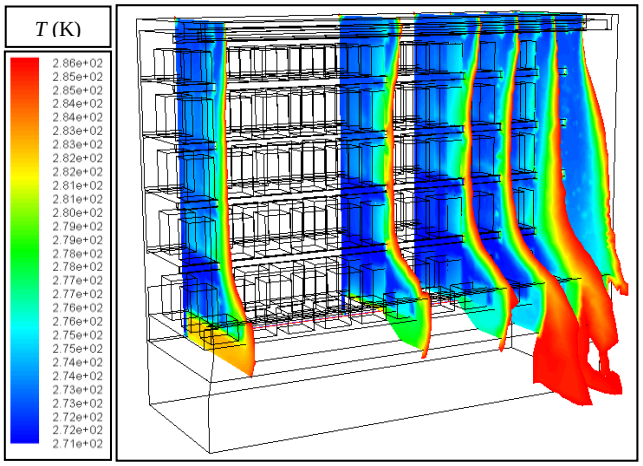

Figure 10: Contours of static temperature at different sections along the cabinet with 0.2 m/s side flow (Cabinet's length 2.45m)

In retail food stores cabinets are arranged in a line-up, which can extend to anything up to 15 meters or more. In the case where a draught is along the face of the cabinet, only 0.45 m out of the 15 m will be affected by the side flow. Therefore, for the most part of the cabinet length the flow can be assumed to be two-dimensional. For this reason, and to save on computational time, a 2D CFD model was employed for the design optimization.

8. Assessing the key factors of energy-efficient display cabinet design

The results show the product temperatures on all the three shelves reaching as high as 8.5°C. There was also a variation in the product temperature distribution from right to left side, the product situated near to the side panel where the cross flow was coming from (right side) have lower temperatures compared with the other sides. The temperature of the product on the front part of the shelves is higher compared to the product on the rear part of the shelf. In general, the failure of this cabinet to meet the performance criteria for this class of cabinet can be attributed to the characteristics of the air curtain and the poor air distribution system of the display cabinet. As indicated earlier, infiltration through the air curtain is the largest constituent of the display cabinet-cooling load. The total performance of the air curtain and the amount of heat transferred across it depends on several factors, including:

- Mass flow rate required by the air curtain
- Air curtain width
- Air curtain velocity
- Discharge angle of the air curtain outlet
- The honeycomb
- The position of the air curtain outlet relative to the front edge of the top shelf

In the following sections, with the aid of the validated CFD model, the above factors will be investigated in detail and the mass flow rate required by the display cabinet will be obtained.

8.1. Optimum total air mass flow rate for open vertical display cabinet

Heat transfer inside the display cabinet involves interactions between the product and the internal environment of the display cabinet. The constituents of heat from the surrounding environment include heat transfer by conduction, radiation and infiltration. Convection is the main heat transfer mechanism that cools the product when chilled air comes into contact with it. Faramarzi [17] described the cooling load of a typical refrigerated display cabinet by the following equation:

$$Q_{case} = [Q_{conduction} + Q_{radiation} + Q_{\inf iltration-sensible} + Q_{lights} + Q_{fan-motor} + Q_{defrost-heater} + Q_{anti-sweat-heater} + Q_{product-pull-down-load}]_{sensible} + [Q_{\inf iltration-latent} + Q_{product-latent}]_{latent} \quad (7)$$

Since the products in vertical multi-deck *cabinets* are normally wrapped, the latent heat transfer component from the product has not been included in this analysis. Heat transfer from the fan motor has also not been considered as the evaporator coil was not incorporated in the modelling. Anti-sweat heaters are normally used on low temperature open display cabinets and cabinets equipped with doors. Chilled food, open, vertical display cabinets are being considered so the anti-sweat heater load was not included in the analysis. The components included in the analysis are conduction, infiltration and radiation as follows:

$$Q_{case} = [Q_{conduction} + Q_{radiation} + Q_{\inf.-sensible}]_{sensible} + [Q_{\inf.-latent}]_{latent} \quad (7)$$

A temperature of 277 K was considered as the maximum product temperature that the product could reach during the simulation. Evaporator coil air-off temperature was set at 271K and a relative humidity of 93 %.

A uniform mass flow distribution was assumed with regard to the air leaving the evaporator. The evaporator coil air off temperature was set at 271 K and this temperature provides a good compromise between airflow requirement and evaporator fan and compressor power consumption [18].

For all conditions, simulations were carried out to determine the mass flow rate required to maintain the maximum product temperature below 278 K. The procedure for determining the required fan flow rate, involved increasing the mass flow rate through the evaporator coil, while monitoring the product temperature in the cabinet. Table 4 shows the variation of the product temperature with the mass flow rate through the evaporator at constant evaporator coil air-off temperature, it can be seen that increasing the airflow through the evaporator coil results in a lower product temperature.

Table 4: Product temperature and cooling load for different air mass flow rate

Mass flow rate (kg/s)	Sh1 (°C)	Sh2 (°C)	Sh3 (°C)	Sh4 (°C)	Sh5 (°C)	Cooling load (kW)
0.316	5.9	4.2	4	4.1	4.8	4.27
0.396	5.2	3.8	3.6	3.8	4.1	4.61
0.434	4.2	3.5	3.4	3.4	3.9	4.73

Airflow of 0.434 kg/s was found to be enough to keep the maximum product temperature around 277 K (4°C). Increasing the air mass flow rate through the evaporator coil whilst keeping the coil air-off temperature constant will result in higher cooling rates in the cabinet. The air and product temperature contours for the different airflow rates are presented in Figure 11. For airflow rate of 0.132 kg/s/m and above, the higher product temperatures were at shelf 1 (bottom) and shelf t (top).

The 2nd, 3rd and 4th shelf product have nearly the same temperature. Increasing the air mass flow rate through the evaporator coil whilst keeping the coil air-off temperature constant will result in higher cooling rates in the cabinet and the cabinet will be able to satisfy higher cooling loads.

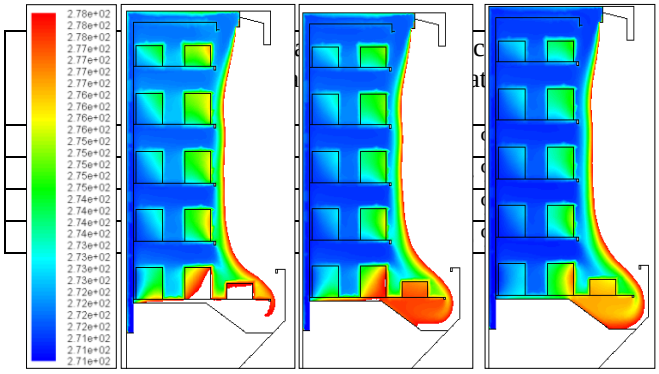

0.132 kg/s.m 0.165 kg/s.m 0.181 kg/s.m

Figure 11: Temperature contours (K)for different airflow rates

8.2. Effect of air curtain slot width on cabinet performance

The ability of the air curtain to seal the cabinet opening area was found to be dependent on the initial momentum of the supplied air and the magnitude of the transverse forces [19]. The deflection modulus is related to the air curtain width, air curtain velocity, height of the opening and the densities of warm and cold air on both sides of the air curtain.

Air curtain widths of 50, 70, 90 and 110 mm were considered and airflow rate of 0.434 kg/s was considered in the simulations. Figure 12 shows the product and air temperature contours inside the display cabinet for different air curtain widths at constant fan flow. It can be seen that the product temperature variation for the cases considered is small. The higher product temperatures are located at the 1st (bottom) shelf and the lowest product temperatures are at 2nd, 3rd and 4th shelves.

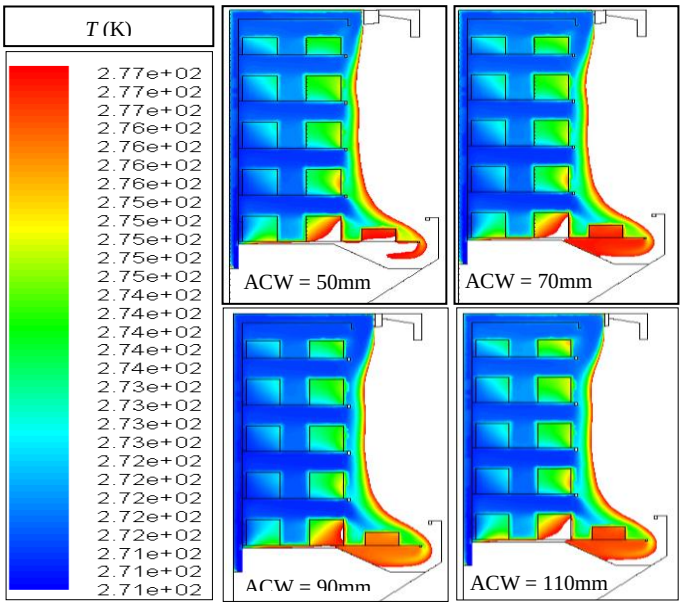

Figure 12: Product temperature contours at different air curtain width (ACW)

ACW (mm)	Minimum air curtain velocity required (m/s)	Average air curtain velocity predicted by CFD (m/s)
50	0.6	0.67
70	0.50	0.55
90	0.45	0.46
110	0.4	0.41

Table 5 shows the product temperature and cooling load variation for different air curtain widths. It can be seen that the effect of air curtain slot width on the product temperature is quite small. The maximum variation on the bottom shelf (shelf 1) was found to be around 1 °C

Table 5: Product temperature and cooling load variation for different air curtain width

Air curtain width (ACW)(mm)	Sh1 (°C)	Sh2 (°C)	Sh3 (°C)	Sh4 (°C)	Sh5 (°C)	Cooling load (kW)
50	4.9	3.7	3.7	3.7	3.7	5.16
70	4.8	3.6	3.5	3.5	3.7	4.80
90	3.8	3.4	3.4	3.4	3.9	4.60
110	3.9	3.5	3.4	3.4	4.1	4.73

Increasing the air curtain slot width resulted in a lower mass flow rate through the perforated back panel and more mass flow rate through the air curtain. At an air curtain slot width of 50 mm the percentage mass flow rate of the air curtain to the total mass flow rate in the cabinet was around 28%. Increasing the air curtain slot width to 70 mm increased the percentage air curtain mass flow rate to 34%.

Increasing the air curtain slot width above 70 mm still resulted in an increase in the mass flow rate through the air curtain but at a much lower rate Table 6.

Table 6: Percentage of air curtain mass flow rate for different ACW

ACW (mm)	Total air curtain mass flow rate (kg/s/m)	AC percentage flow rate (%)
50	0.052	28 %
70	0.062	34 %
90	0.064	35 %
110	0.066	36 %

8.3. Air curtain velocity (ACV)

The sealing ability of an air curtain depends on its initial momentum and the size of transverse forces, against which the air curtain is attempting to seal. The dimensionless ratio of these two forces is known as the deflection modulus [19].

$$D_m = \frac{\rho_o . b_o . U_o^2}{g.H^2.(\rho_c - \rho_w)} \qquad \text{----------(9)}$$

Since at a given atmospheric pressure the air density is inversely proportional to the absolute temperature, Equation 9 may also be written as:

$$D_m = \frac{b_o . U_o^2}{g.H^2\left[\left(\frac{T_o}{T_c} - \frac{T_o}{T_w}\right)\right]} \qquad \text{----------(10)}$$

The velocity required for such an air curtain to provide a good seal is:

$$U_o^{\ 2} = \frac{D_m . g.H^2\left(\frac{T_o}{T_c} - \frac{T_o}{T_w}\right)}{b_o} \qquad \text{----------(11)}$$

For a range of H / b_o, [19], determined the minimum value of D_m for good sealing to be between 0.14 and 0.18. For H / b_o in the range between 16 and 64 the value of D_m can be determined from:

$$D_m = 0.257(H / b_o)^{-0.1336} \qquad \text{----------(12)}$$

The initial velocity of the air curtain can then be determined from:

$$U_o^{\ 2} = \frac{0.257(H / b_o)^{-0.1336} . g.H^2\left(\frac{T_o}{T_c} - \frac{T_o}{T_w}\right)}{b_o} \qquad \text{---(13)}$$

For values of H / b_o lower than 16, a deflection modulus of 0.18 can be used and the equation below can be applied to determine the initial air curtain velocity:

$$U_o^{\ 2} = \frac{0.18 . g.H^2\left(\frac{T_o}{T_c} - \frac{T_o}{T_w}\right)}{b_o} \qquad \text{-----(14)}$$

In order to achieve stable operation, the air curtain momentum should always be slightly above the minimum value determined by the deflection modulus. For application to refrigerated display cabinets, equation 13 and 14 can be used by replacing H (opening height) with the maximum shelf-height available in the display cabinet [12].

Air curtain velocity variation for different air curtain widths can be found in Figure 13, where a low air curtain velocity is shown at a large air curtain width and high air curtain velocity at a small air curtain width.

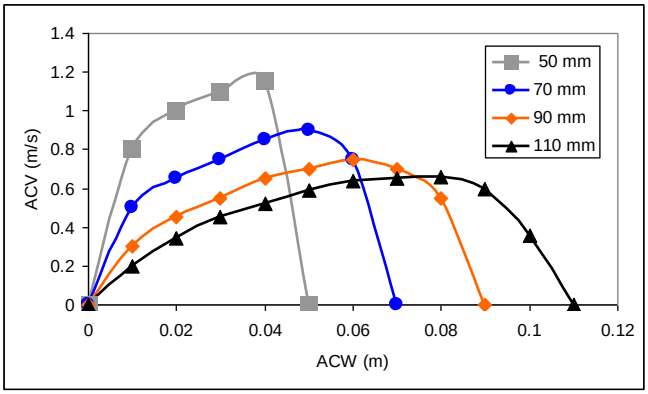

Figure 13: Air curtain velocity predicted by the CFD modelling at different ACW

Table 7 shows that for 50 , 70 , 90 and 110 mm widths the average air curtain velocity is slightly higher than the required (according to Hayes [19]) to provide good sealing for the environment of the display cabinet.

The results of the CFD modelling showed that air curtain widths of 90 and 110 mm ensure the required air curtain velocity.

ACW (mm)	Minimum air curtain velocity required (m/s)	Average air curtain velocity predicted by CFD (m/s)
50	0.6	0.67
70	0.50	0.55
90	0.45	0.46
110	0.4	0.41

Table 7: Comparison of the air curtain velocity predicted by the CFD model with the required values calculated from Eq. 14.

8.4. Effect of the discharge angle on the performance of the air curtain

At an air curtain width of 90 mm, simulations were carried out to investigate the effect of the discharge angle of the air curtain on its performance. Product on the top shelves were the most effected by the discharge angle with a maximum variation of 0.5°C and product on the lower shelves were less affected by the discharge angle. The cooling load of the cabinet is also slightly affected by the discharge angle of the air curtain. Table 8 shows that lower cooling load was obtained at discharge angle ranging between 5° and 10°.

Table 8: Effect of the discharge angle on the cooling load

Discharge angle	Cooling load (kW)
0°	4.57
5°	4.54
10°	4.56
12°	4.60
15°	4.63

8.5. Effect of using honeycomb in the air curtain on the performance of the display cabinet

Honeycomb has been reported to be important for the performance of air curtains. It can improve the uniformity of flow and can reduce the initial turbulence of the air curtain. The Carter cabinet was already equipped with a honeycomb. To provide a real picture of the flow at the air curtain outlet a true modelling of the honeycomb was implemented. Velocity vectors for a cabinet with and without honeycomb are shown in Figure 14. It can be seen that using honeycomb provides a more uniform air curtain.

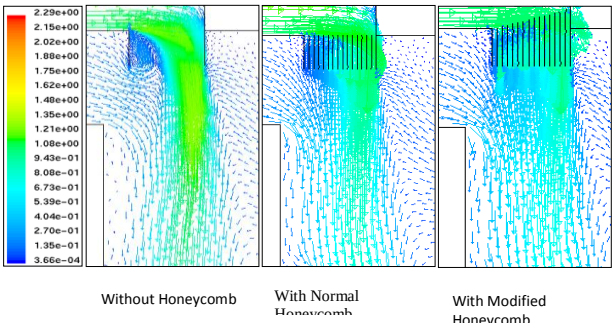

Figure 4: Effect of using honeycomb on the air curtain velocity distribution at the air curtain outlet

Using the modified shaped honeycomb the airflow shows more uniformity and a slightly wider air curtain. Also it can be seen that the velocity at the air curtain outlet is higher without honeycomb than with honeycomb. The mass flow rate of the air curtain is concentrated more to the outer half of the air curtain (the half of the air curtain outlet nearer to the outside of the display cabinet). Using honeycomb provides a better distribution of the mass flow rate at the air curtain outlet.

When using a modified shaped honeycomb, a more uniform distribution of airflow is obtained. The percentage difference of the mass flow rate through the air curtain for the cases of the display cabinet with and without honeycomb was found to be around 0.4%, which could be considered negligible.

Results from Figure 14 prove that providing a uniform velocity distribution at the air curtain outlet, which leads to more uniform flow leaving the air curtain; can optimise the performance of the air curtain. Using a modified shaped honeycomb showed that the performance of the air curtain has been further improved.

The CFD results showed that the optimum air curtain performance was obtained when the air curtain velocity was uniform at the outlet of the air curtain. The effect of using a honeycomb on the product temperature was not significant but a saving of around 4 % in the cooling load was achieved.

8.6. Position of the air curtain outlet relative to the front edge of the top shelf

The validated 2-D CFD was used to investigate the effect of the air curtain position on the performance of the display cabinet at a constant evaporator coil air-off mass flow rate (0.181 kg/s/m) and evaporator coil air-off temperature of 271 K. Figure 15 shows path lines coloured by static temperature for three cases: distance between the front edge

of the top shelf and the air curtain outlet of 0, 50 and 100 mm.

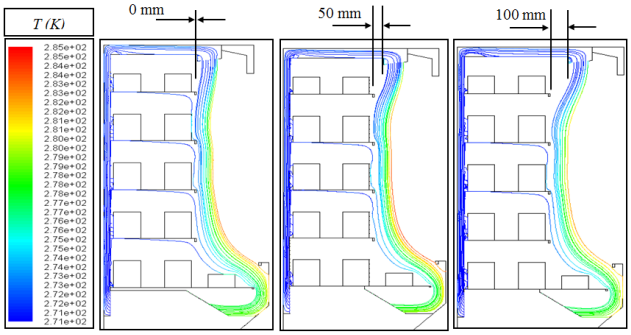

Figure 15: Path lines coloured by static temperature for different positions of air curtain outlet

When the distance is zero it can be seen that the air curtain discharges nearly vertically downwards along the face of the cabinet, constrained by the product on the shelves and forming two mixing zones: an inner zone (inside the cabinet) and an outer zone (outside the cabinet). In the region adjacent to the surrounding air (outer zone), the air curtain airflow mixes with the ambient warm air, which is drawn into the flow going towards the return air grille. Accordingly, the temperature of the air in the air curtain increases gradually due to the entrainment of ambient air.

When the distance of the air curtain outlet from the front edge of the shelves increases, the air curtain starts to deflect inwards towards the cabinet. This leads to a longer air curtain jet, from air curtain outlet to return air grill, which results in a longer area in which ambient air entrainment and mixing can take place. Increased ambient air entrainment leads to a higher thermal load and a higher product temperature.

Figure 15 shows that the path lines of the air curtain in the case when the position of the air curtain outlet is on the same vertical line as the front edge of the shelves is slightly colder (inner zone) compared to the other two cases.

The CFD results showed that increasing the distance between the front edge of the top shelf and the air curtain outlet by 100 mm increased the cooling load by around 2% and the product temperature was slightly higher.

9. Cabinet modifications

Based on the results of the of the CFD model, the display cabinet was retested with the following modifications:

- The display cabinet was fitted with 6 evaporator fans to increase the air mass flow rate up to 0.434 kg/s. The required supply glycol temperature to keep the air-off temperature at around -2°C was found to be -7°C at a volume flow rate of 0.8 (m^3/h).
- Air curtain width was changed to 90 mm instead of 110 mm.
- The display cabinet was already fitted with a honeycomb.
- Air curtain discharge angle was reduced to around 8° instead of 12°

The mass flow rate of the display cabinet was assessed based on measuring the average velocity at the evaporator coil air–off section and multiplying this value by the cross section area of the evaporator coil air–off section and density of the air. The mass flow rate through the air curtain was controlled by controlling the perforation rate of the perforated back-panel.

Figure 16 shows the product temperature variation before and after the modifications suggested by the CFD models to the display cabinet.

It is clear that the changes that were made to the display cabinet contributed to reducing the product temperature to the required value. Moreover, the results show a good agreement with data predicted by the CFD model, except the bottom shelf where the middle-top product was slightly above 4°C.

10. Conclusions

The computational work and measurements indicated that the flow for most of the cabinet's length is predominantly two-dimensional. Therefore, two- dimensional CFD models were used to optimize the display cabinet.

1. Deflection modulus equation established by [19] can be adapted for the applications of the vertical multi-deck display cabinets by replacing H (high of the opening) with maximum shelf-height available in the display cabinet.

2. The optimum air curtain mass flow rate was found to be around a third of the total mass flow rate in the cabinet. The rest of the flow is divided between the shelves depending on the design of the display cabinet.

3. Minimising the distance between the air curtain outlet and the front edge of the top shelf provided better protection to the air and products in the display cabinet. An air curtain slot width of between 90 mm and 110 mm was found to provide best performance for the cabinet considered in the investigations. Inclining the air curtain outwards by between 5° and 10° provided the best protection from the environment in the display cabinet .

4. The use of a honeycomb at the air curtain discharge provided better performance than without a honeycomb. Using a modified honeycomb, to increase flow resistance and make the air velocity through the air curtain more uniform, improved the air curtain performance further, resulting in around 4% reduction in the cooling load of the cabinet.

Despite efforts to increase the efficiency of air curtains in display cabinets, infiltration of ambient air into the cabinet still accounts for over 70% of the total cabinet load. Therefore improving the performance of air curtains should be a priority in the design of open display cabinets as it will reduce both refrigeration energy consumption and the 'cold aisle' effect in retail food stores [20].

References

[1] Y.Chen, G.Chen, X.Yuan, L.Yuan. Experimental study of the performance of single-band air curtains for a multi-deck refrigerated display cabinet, Journal of Food Engineering, 69, (2005) 261-267.

[2] D.A.Paola, C.Giovanni, C.Giulio. Two- and three-dimensional CFD applied to vertical display cabinets simulation, International Journal of Refrigeration, 29, (2006) 178-190.

[3] J.A.Evans, S.Scarceli, M.V.L. Swain. Temperature and energy performance of refrigerated retail display and commercial catering cabinets under test conditions, International Journal of Refrigeration, 30, (2007) 398-408.

[4] A.Hadawey. Design of chilled food display cabinets for better temperature integrity and longer product shelf life. PhD Thesis. 2006. Brunel University.
Ref Type: Thesis/Dissertation

[5] W.Xiang, S.A.Tassou. A dynamic model for vertical multideck refrigerated display cabinets. IIR Proceedings Series" Refrigeration Science and Technology", 637-644. 1998.
Ref Type: Conference Proceeding

[6] International Organization for Standardization. ISO 23953-2(Refrigerated Display Cabinets-Part 2: Classification, requirements and test conditions.). 2005.
Ref Type: Bill/Resolution

[7] Y.Ke-zhi, D.Guo-liang, C.Tian-ji. Simulation of air curtains for vertical display cases with a two-fluid model, in: Applied Thermal Engineering, 27, (2007), 2583-2591.

[8] G.Cortella. CFD aided retail cabinets design, in: Compute Electron Agric.34, (2002), 43-66.

[9] T.H.Lan, D.H.T.Gotham, M.W.Collins. A numerical simulation of the air flow and heat transfer in a refrigerated food display cabinet. Second European Thermal Science and 14th UIT National Heat Transfer Conference. (1999), 1139-1146.
Ref Type: Conference Proceeding

[10] J.N.Baleo, L.Guyonnaud, C.Solliec. Numerical simulations of air flow distribution in a refrigerated display case air curtain. Proceedings of 19th International Congress on Refrigeration.2,(1995),681-687. Ref Type: Conference Proceeding

[11] BS 6148: British standard methods of test for commercial refrigerated cabinets. 1981.
Ref Type: Bill/Resolution

[12] W. Xiang. Investigation and optimization multi-deck display cabinet and retail store environment. PhD Thesis. 2004. Brunel University.
Ref Type: Thesis/Dissertation

[13] D.Stribling, S.A.Tassou, D.Marriot. A tow-dimensional CFD model of a refrigerated display case, ASHRAE Transactions, 103, (1997) 88-94.

[14] W.S.Atkins. Chilled multideck cabinet airflow study. Report for Safeway Stores PLC, UK, 31 p. 1992.

[15] A.M.Foster, M.Madge, J.A.Evans. The use of CFD to improve the performance of a chilled multi-deck retail display cabinet, International Journal of Refrigeration, 28, (2005) 698-705.

[16] D.Marriot, D.Stribling, S.A.Tassou. Optimization of the design of refrigerated display cases using computational fluid dynamics. Proceedings of the Institute of Refrigeration 92, (1996), 7.1-7.7.
Ref Type: Conference Proceeding

[17] R. Faramarzi. Efficient display case refrigeration, ASHRAE Journal, 6, (1999), 46-52.

[18] S.A.Tassou, A.Maki. Design optimization evaluation methodology of vertical multi-deck display cabinets. TTR International Conferences, Vicenza. 2005.
Ref Type: Conference Proceeding

[19] F.C.Hayes. Heat transfer characteristics of air curtain, ASHRAE Transactions, (1969) 153-167.

[20] Air Curtain Design Optimization in Refrigerated Open Vertical Display Cases. PAC Winter 2008 Meeting, New York

[21] I Gary, P. Luscombe, L. Mclean, C.S.P. Sarathy, P. Sheahen, and K. Srinivasan. Improvement of air distribution in refrigerated vertical open front remote Supermarket display cases. International Journal of Refrigeration 31, (2008), 902-910.

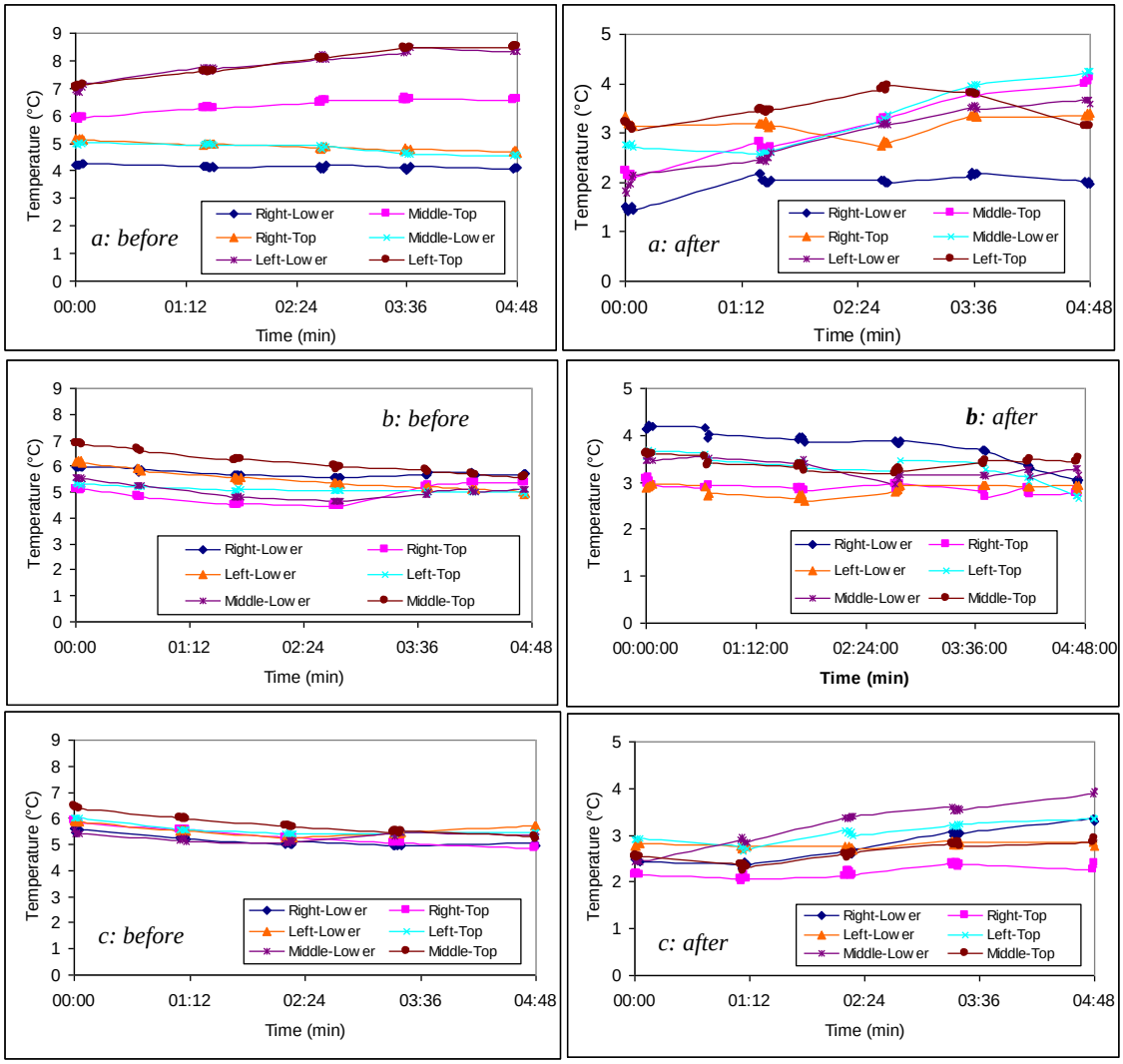

Figure 16: Product temperature variation before & after the cabinet's modifications
(a: bottom shelf "Shelf 1", b: third shelf "shelf 3", c: top shelf "shelf 5")